Effect of Electric Potential and Mechanical Force on Copper Electro-Chemical Mechanical Planarization

2012 Jpn. J. Appl. Phys. 51 036504

(http://iopscience.iop.org/1347-4065/51/3R/036504)

Japanese Journal of Applied Physics **51** (2012) 036504 **REGULAR PAPER**
DOI: 10.1143/JJAP.51.036504

Effect of Electric Potential and Mechanical Force on Copper Electro-Chemical Mechanical Planarization

Sheng-Wen Chen[1], Te-Ming Kung[1], Chuan-Pu Liu[1], Shih-Chieh Chang[2], Yi-Lung Cheng[3], and Ying-Lang Wang[2]*

[1]*Department of Material Science and Engineering, National Chen-Kung University, Tainan 701, Taiwan, R.O.C.*
[2]*Institute of Lighting and Energy Photonics, National Chiao Tung University, Hsinchu 30050, Taiwan, R.O.C.*
[3]*Department of Electrical Engineering, National Chi Nan University, Nantou 545, Taiwan, R.O.C.*

Received September 15, 2011; accepted December 30, 2011; published online March 5, 2012

In this study, the dependence of Cu electrochemical mechanical planarization (ECMP) rate on electric potential and mechanical force in electrolyte is investigated using potentiodynamic analysis, electrochemical impedance spectroscopy (EIS), and X-ray photoelectron spectroscopy (XPS). In chemical etching, CMP, electropolishing, and ECMP processes, the Cu removal rate is mainly affected by the interplay between electric potential and mechanical force. An equivalent circuit is built by fitting the EIS results to explain the behavior of Cu dissolution and Cu passive film. The Cu dissolution rate increased with decreasing charge-transfer time-delay. The resistance of the Cu passive film (R_p) is proportional to the intensity ratio of $Cu_2O/[Cu(OH)_2 + CuO]$.

1. Introduction

The planarization of copper (Cu) damascene structures is becoming increasingly challenging due to the ongoing reduction of feature sizes, along with high packing density, use of ultra-low-*k* dielectrics, and an increasing number of interconnect layers in silicon integrated circuits.[1,2] The chemical mechanical planarization (CMP) technique is limited for such applications, with major problems being instability of slurries, scratches generated on surfaces, various metal contaminants, dishing features, post-cleaning difficulties, selectivity problems, and high cost of equipment and maintenance.[3–9] The material integration difficulties described above for Cu CMP with porous low-*k* dielectrics have led researchers to investigate alternative planarization processes such as electro-polishing and electrochemical mechanical planarization (ECMP). ECMP appears to be a viable approach for the efficient planarization of ultra low-*k* structures and fulfill the strict technical limitations.[10–14] ECMP combines aspects of two technologies, namely CMP and electropolishing.[15] During polishing, a passive film, such as an oxide film, is formed at high electric potentials and is then removed by mechanical wearing.[10,16–19] The factors that affect ECMP include characteristics of the solutions,[20–22] electric potential, and mechanical force.[10,23] The Cu removal rate for ECMP has been demonstrated to be linearly proportional to electric potential.[10] However, at the present time, little is known about ECMP in general,[10,11,13,15,20–23] especially its surface reactions and dissolution/polishing mechanisms. In order to obtain an appropriate Cu metallization process, the effect of electric potential and mechanical force in the electrolyte for Cu-ECMP processes should be investigated. In this paper, the relationship between polishing conditions and the ECMP removal rate is examined in depth and an equivalent circuit is established to explain the dissolution and polishing behaviors of a Cu film in an H_3PO_4 electrolyte using electrochemical impedance spectroscopy (EIS). The structure of the Cu surface after ECMP is analyzed using X-ray photoelectron spectroscopy (XPS).

*E-mail address: ylwang@tsmc.com

2. Experimental Procedure

The experiments were performed at room temperature in a three-electrode cell constructed from a 350-mL cubic cell made of poly(vinyl chloride) (PVC) material, a 7-cm^2 blanket wafer as the working electrode, a 7-cm^2 platinum plate as the counter electrode, and an Ag/AgCl reference electrode in a 3 mol/L KCl saturated solution. The blanket wafer was prepared by depositing a 30-nm-thick sputtered TaN diffusion barrier followed by a 100-nm-thick Cu seed layer on a 200-nm-thick SiO_2/Si(100) substrate. Subsequently, a Cu film was electroplated to a thickness of 1.1 μm in a solution consisting of 0.25 mol/L $CuSO_4 \cdot 5H_2O$, 1.0 mol/L sulfuric acid, and 50 ppm chloride ions. The ECMP operating conditions were: electric voltages ranged from 300 to 1800 mV vs Ag/AgCl, down force ranged from 0.07 to 70 psi, and the rotation speed ranged from 50 to 800 rpm. Soft polishing pads (Rodel Politex pad) were used in the ECMP process. The polishing pads were porous to let the electrolyte (85 wt % H_3PO_4) through, creating effective electrical pathways between the counter electrode, reference electrode, and working electrode. The cross-sections of polished Cu films were imaged using a field emission scanning electron microscope (FESEM; Hitachi S4800) operated at 15 kV. Electrochemical analyses, including *in-situ* current-time and potentiodynamic tests, were performed with a variable speed rotator [636 rotating disk electrode (RDE)] and PARSTAT 2273 controlled by PowerCORR software (Princeton Applied Research) in a three-electrode cell. EIS measurements were performed at 300, 500, 800, and 1800 mV versus open circuit potential, and conducted by superimposing an AC signal with an amplitude of ±20 mV in the frequency range of 100 kHz to 1 Hz. The equivalent circuit was established and simulated using ZSimpWin version 3.1 with EIS data. XPS was acquired with a VG Scientific Microlab photoelectron spectrometer at a base pressure below 1×10^{-8} Torr using Mg Kα radiation (1253.6 eV). The time needed for each data point in a single scan was 0.1 s, and the data interval was 0.1 eV. The absolute binding energies of various surface species were calibrated using the C 1s line at 285.3 eV. The inelastic background was removed from the spectra using Shirley's method.[24]

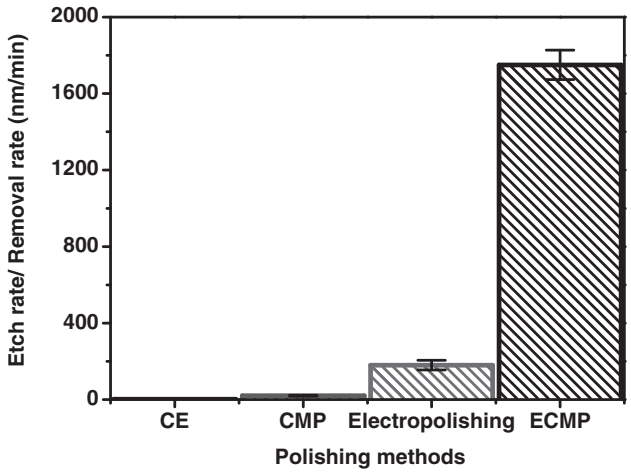

Fig. 1. Cu removal rate for chemical etching (CE), chemical mechanical planarization (CMP), electroploishing, and electrochemical mechanical planarization (ECMP).

Table I. Operation conditions of electric potential and mechanical force for chemical etching (CE), chemical mechanical planarization (CMP), electro-ploishing, and electrochemical mechanical planarization (ECMP).

	Electric voltage (mV)	Down-force (psi)	Speed of rotation (rpm)	Solution
CE	0	0	0	85 wt % H_3PO_4
CMP	0	0.14	200	85 wt % H_3PO_4
Electro-polishing	800	0	200	85 wt % H_3PO_4
ECMP	800	0.14	200	85 wt % H_3PO_4

3. Results and Discussion

A comparison of the etching/removal rates of a Cu film for chemical etching (CE), CMP, electropolishing, and ECMP is shown in Fig. 1. The polishing conditions are listed in Table I. ECMP was decomposed into CE, CMP, and electropolishing to better understand its mechanisms. 85 wt % H_3PO_4 was used as the oxidant (for CE and CMP) and electrolyte (for electropolishing and ECMP) in the experiments. Politex polishing pads with a down force of 0.14 psi were employed in CMP and ECMP. In Fig. 1, ECMP has the highest Cu removal rate. The percentages of the ratios of the Cu removal rate of CE, CMP, and electropolishing to that of ECMP are 0.1, 1.1, and 10.3%, respectively. For static etching, it is difficult to quickly corrode Cu films in a weak acid (H_3PO_4). The removal rate of ECMP is much higher than the sum of the other polishing methods, implying that the effects in combination have a much larger impact on the total removal rate than they do individually.

Figure 2(a) shows the relationship between current density (I_d) and electric voltage against the reference electrode (Ag/AgCl) during ECMP and electropolishing. I_d indicates that Cu metal was dissolved; it is produced at the anode surface at the given potential. In Fig. 2(a), the curve for ECMP was obtained at a rotation speed of 200 rpm with a down force of 0.14 psi, whereas the curve for electropolishing was obtained at a rotation speed of 200 rpm without down force. The negative slope of I_d for electropolishing implies that the Cu removal rate decreased with increasing electric potential, which is due to the formation of a passive film.[25,26] In contrast, I_d increases with increasing electric potential for ECMP because the passive film is removed by mechanical force, which includes the down force and rotation speed, upon formation. Therefore, the combined effects of the mechanical force and electric potential become more obvious at higher potentials. Figure 2(b) shows the Cu removal rate as a function of electric potential, down force, and rotation speed in a H_3PO_4 electrolyte in ECMP, with the other two variables kept constant. It was found that the effect of electric potential on the Cu removal rate of ECMP is more significant than that of the mechanical force. This result is due to the Cu dissolution rate being high at high electric potentials.

Figure 2(c) shows the potential dynamic curves obtained for ECMP by scanning the potential (at 20 mV/s) at down forces of 0 to 70 psi. The curve at 0 down force is typical for a passive metal, featuring a dissolution peak at ~0.03–0.7 V, a passivation plateau at ~0.7–1.6 V, and pit generation followed by O_2 evolution for high anodic potentials (above 1.6 V).[25,26] The current density thus decreases with increasing electric voltage in Fig. 2(a). For curves with a nonzero down force, the passivation plateau region disappears. I_d increases with increasing down force at potentials above 0.2 V. For example, when $E = 0.3$ V vs Ag/AgCl, as shown in the inset of Fig. 2(c), I_d slightly increases from 43.7 to 53.8 mA/cm^2 as the down force increases from 0.07 to 70 psi. Rotation speed is also factor in the mechanical force. Figure 2(d) shows the potential dynamic curves of the Cu disk electrode for rotation speeds of 50 to 800 rpm under a down force of 0.14 psi in a H_3PO_4 electrolyte. In Fig. 2(d), I_d increases with the rotation speed at potentials above 0.2 V. For example, when $E = 0.3$ V vs Ag/AgCl, as shown clearly in the inset of Fig. 2(d), I_d slightly increases from 29.4 to 38.0 mA/cm^2 as the rotation speed increases from 50 to 800 rpm. The increase of I_d is consistent with the results shown in Fig. 2(b).

Figures 3(a)–3(c) shows the Nyquist plots of the Cu films as a function of electric potential, down force, and rotation speed and Cu polished in a H_3PO_4 electrolyte for ECMP, respectively; the other two variables were kept constant. In the Nyquist plots, the y-axis is the imaginary impedance (reactance) and the x-axis is the real impedance (resistance) in the equivalent circuit associated with the ECMP system. All the plots show two semicircles, one on the left at high frequencies (>1000 Hz) one on the right at low frequencies (<0.1 Hz). The possible chemical reactions of a Cu film in a H_3PO_4 electrolyte are as follows:[26–28]

$$\mathrm{Cu(S)} \rightarrow \mathrm{Cu^+ + e^-}, \quad (1)$$

$$\mathrm{Cu(S)} \rightarrow \mathrm{Cu^{2+} + 2e^-}, \quad (2)$$

$$\mathrm{2Cu^+ + H_2O} \rightarrow \mathrm{Cu_2O + 2H^+}, \quad (3)$$

$$\mathrm{Cu^+ + 2OH^-} \rightarrow \mathrm{Cu(OH)_2}, \quad (4)$$

$$\mathrm{Cu_2O + H_2O} \rightarrow \mathrm{2CuO + 2H^+ + 2e^-}, \quad (5)$$

$$\mathrm{Cu + H_3PO_4 + H_2O} \rightarrow \mathrm{[CuOH]^+[H_2PO_4]^- + 2H^+ + 2e^-}. \quad (6)$$

The high frequency loop is attributed to the charge-transfer resistance and double-layer capacitance from reactions (1) and (2) and the low frequency loop is attributed to the convective and diffusive mass transport of Cu_2O, $Cu(OH)_2$, and CuO at the surface from reactions (3)–(6) in accordance with previous reports.[27–29] Furthermore, the

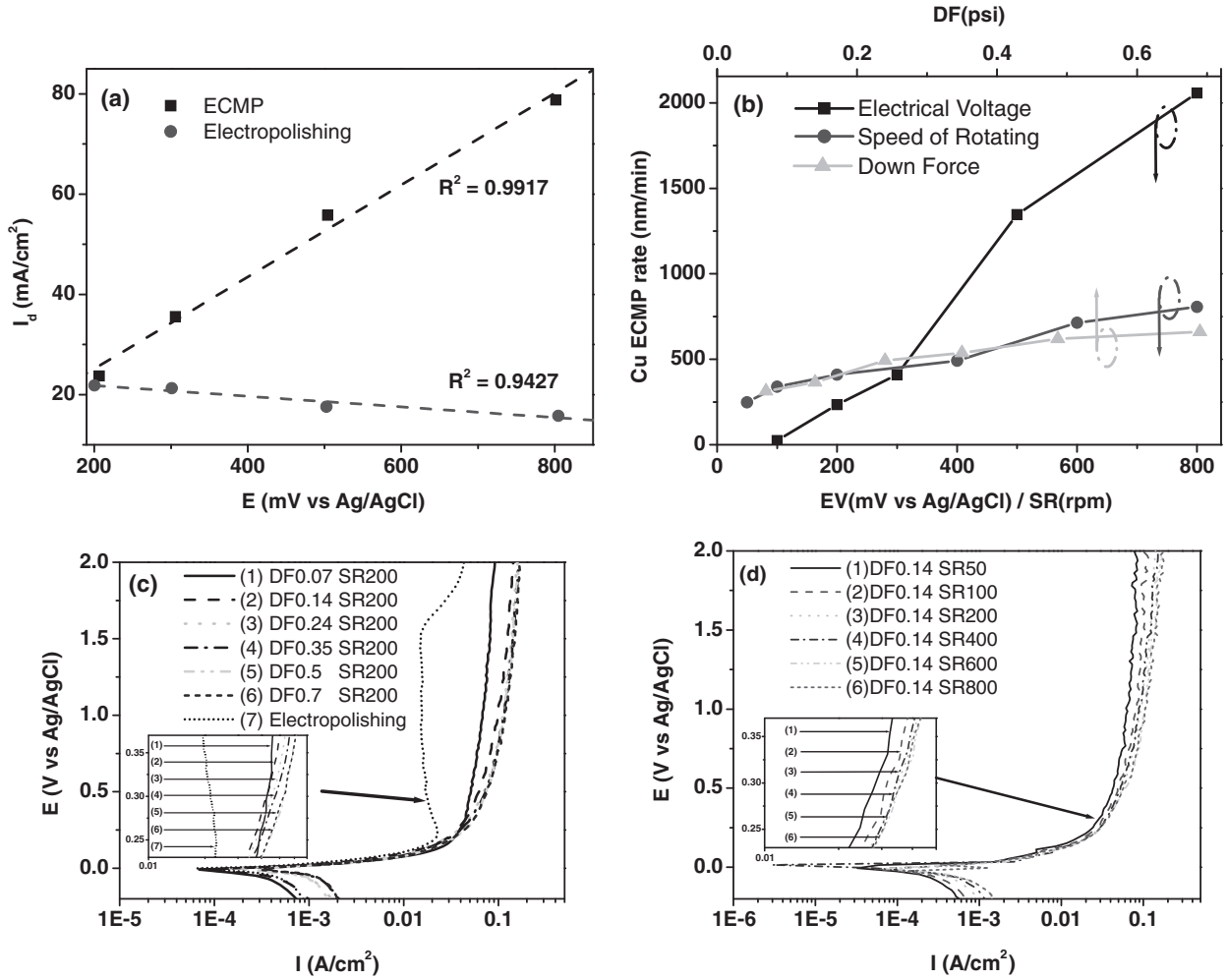

Fig. 2. (a) Linear relationship between current density (I_d) and electric potential against a reference electrode (Ag/AgCl) during ECMP and electropolishing. The conditions of the down-force and the rotation speed were shown in Table I. (b) Cu ECMP rate as a function of electric potential (EV), down-forces (DF) and speeds of the rotating (SR) in a H_3PO_4 electrolyte, where the two variables were kept constant. (c) Potential dynamic curves of Cu disk electrode for various values of DF [(1) 0.07, (2) 0.14, (3) 0.24, (4) 0.35, (5) 0.5, (6) 0.7, and (7) 0 psi] in a H_3PO_4 electrolyte. The disk was rotated at 200 rpm. (d) Potential dynamic curves of Cu disk electrode for various values of SR [(1) 50, (2) 100, (3) 200, (4) 400, (5) 600, and (6) 800 rpm] in a H_3PO_4 electrolyte. DF was 0.14 psi. The potential was scanned at 20 mV/s (c) and (d).

capacitive loop observed in the high frequency range is related to the relaxation of the double layer since its charging–discharging is a very rapid process.[30] In brief, there are two steps for the chemical reactions in the Cu ECMP process: (i) Cu metal is dissolved and ionized [e.g., Cu^+, Cu^{2+}] by charge-transfer reactions with the electrolyte at a given applied electric potential (the first semicircle of the Nyquist plot), (ii) Cu^{2+} and Cu^+ complexes diffuse to the surface of the Cu film and react with O^{2-} and OH^- species to form a temporary passive film [e.g., Cu_2O, CuO, $Cu(OH)_2$], as a diffusion layer, on the Cu surface.

Figure 3(d) shows the simulated equivalent circuit of the Cu ECMP system obtained using ZSimpWin. The best fit was obtained by matching to the result of the EV800DF0.14SR200 case in Fig. 3(a). In Fig. 3(d), R_s is the bulk solution resistance; C_{dl} is the double-layer capacitance of surface reductions; R_{ct} is the charge-transfer resistance (associated with the double layer); C_p is the passivative-capacitance of the adsorption layer; and R_p is the resistance of the passive layer. In this circuit, the RC element of the double layer and the RC element of the passive film are not in series because the passive film is porous. R_{ct} and R_p are in series because the dissolution of Cu films occurs before the formation of the passive film on the surface,[31] which are characterized by the left and right semicircles in the Nyquist plots of Fig. 3(d), respectively. The best-fitted data to Figs. 3(a)–3(c) for all the circuit components are summarized in Table II. CPE_p is the impedance in the constant phase element (CPE) of the Cu passive layer. The values of the system's capacitances can be obtained from CPE phase angle using[32–34]

$$C_p = \frac{(Q_p \times R_p)^{(1/n_p)}}{R_p}, \tag{7}$$

where Q_p is the admittance and n_p is defined as the phase angle of the CPE impedance independent of the frequency, which is also characterized by the degree of non-ideality in the behavior of a capacitor.[30,35] The C_p values of the passive layers are listed in Table II. The table shows that R_p and R_{ct} increase, whereas C_p and C_{dl} decrease with increasing electric voltage (in the range of 300 to 800 mV). The low C_p and high R_p obtained at high potential indicates a thick passive layer formation assuming a fixed dielectric constant for the passive film. The Cu dissolution rate increased with

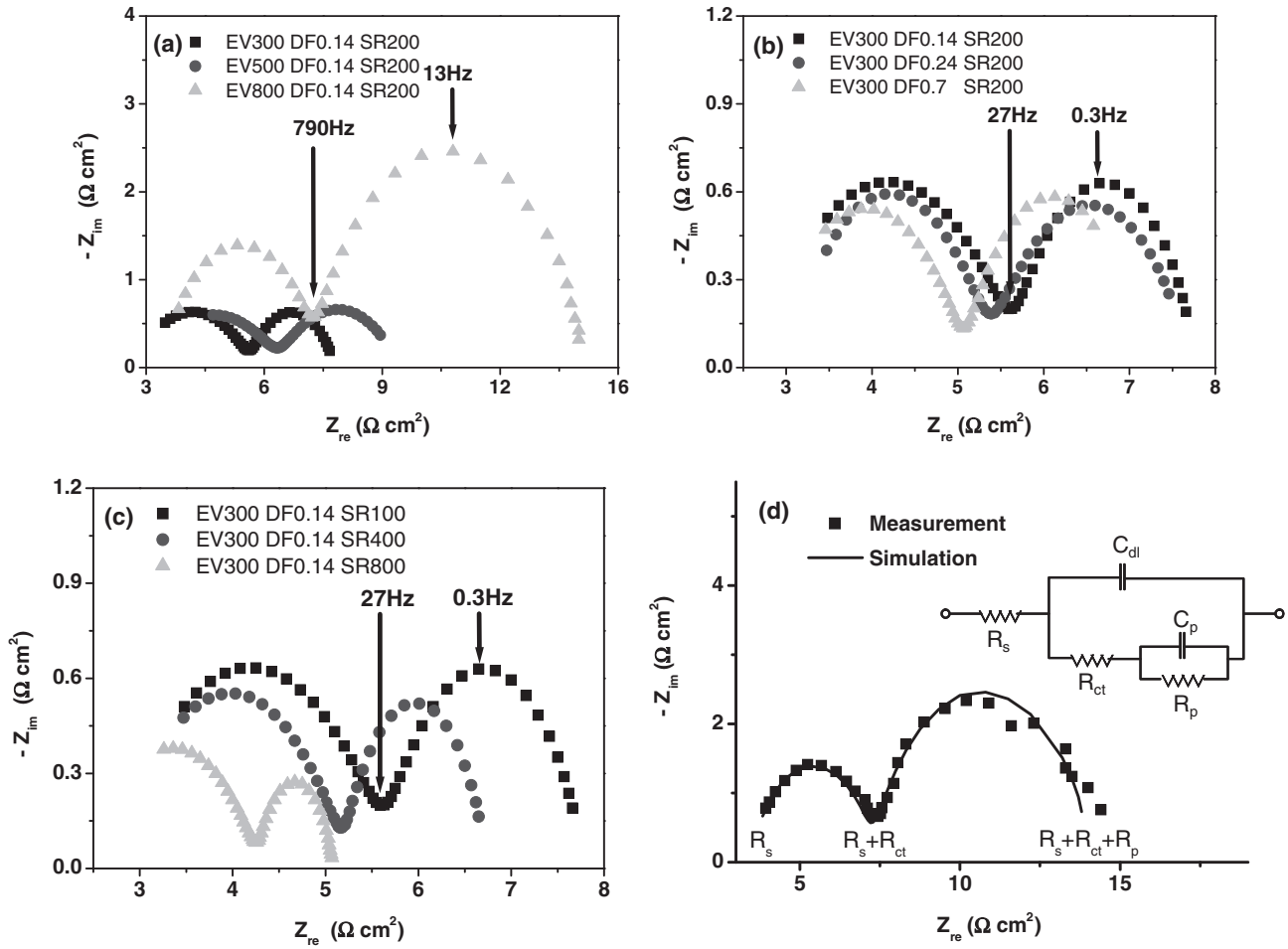

Fig. 3. (a) Nyquist plots of Cu films polished at various electric potentials (EV) in H_3PO_4 electrolyte, (b) Nyquist plots of Cu films polished at various down-forces (DF) in H_3PO_4 electrolyte, (c) Nyquist plots of Cu films polished at various speeds of rotation (SR) in H_3PO_4 electrolyte, and (d) simulation results from the proposed equivalent circuit diagram that was matched with the impedance data of EV800DF0.14SR200 in (a). Proposed equivalent circuit diagram shows the electrochemical characteristics during ECMP in the electrolyte, where R_s is the bulk solution resistance, C_{dl} is the double-layer capacitance, C_p is the passive-layer capacitance, R_{ct} is the charge-transfer resistance (associated with double layer), and R_p is the passive resistance of Cu film.

Table II. Element values of equivalent circuit in Fig. 3(d) required for the best fitting of impedance spectra in Figs. 3(a)–3(c).

Polishing conditions	R_s ($\Omega\,cm^2$)	R_{ct} ($\Omega\,cm^2$)	C_{dl} ($\mu F\,cm^{-2}$)	RC (μs)	R_p ($\Omega\,cm^2$)	CPE_p		C_p ($F\,cm^{-2}$)
						Q_p ($\Omega^{-1}\,cm^{-2}$)	n_p	
EV300 DF0.14 SR200	3.01	2.58	19.12	49.3	2.29	0.32	0.61	0.261
EV500 DF0.14 SR200	3.02	2.96	4.67	13.8	2.33	0.31	0.64	0.2521
EV800 DF0.14 SR200	3.46	3.85	2.7	10.4	6.85	0	0.79	0.0017
EV300 DF0.35 SR200	2.7	2.55	8.93	22.8	1.78	0.34	0.67	0.2622
EV300 DF0.7 SR200	2.55	2.56	7.24	18.5	1.65	0.46	0.68	0.4054
EV300 DF0.14 SR400	2.97	2.18	10.64	23.2	1.58	0.35	0.7	0.2672
EV300 DF0.14 SR800	2.87	1.4	11.02	15.4	0.77	0.36	0.87	0.2952

decreasing charge-transfer time-delay, which is defined as $R_{ct} \cdot C_{dl}$. In Table II, the charge-transfer time-delay greatly decreased when the electric potential was increased from 300 to 800 mV, indicating that the Cu dissolution rate increases with electric potential for Cu ECMP. At a low voltage (300 mV), the charge-transfer time-delay decreased slightly with increasing down force and rotation speed, indicating that the Cu dissolution rate also increases with mechanical force. The value of R_p decreases and C_p increases from 0.07 to 70 psi, implying that the passive layer on the Cu surface becomes thinner. The same results were obtained for rotation speed. The thickness of the passive layer with a high down force or rotation speed can be continuously reduced at low potential, especially for high rotation speeds. The Cu removal rate may be limited to 800 nm/min at low electric potential, as shown in Fig. 2(b). However, the effect of electric potential is greater than that of mechanical force.

Since electric potential greatly affects the Cu removal rate, it was increased in the following experiment. Figure 4

Table III. Element values of equivalent circuit in Fig. 3(d) required for the best fitting of impedance spectra in Fig. 4.

Polishing conditions	R_s ($\Omega\,cm^2$)	R_{ct} ($\Omega\,cm^2$)	C_{dl} ($\mu F\,cm^{-2}$)	RC (μs)	R_p ($\Omega\,cm^2$)	CPE_p		C_p ($F\,cm^{-2}$)
						Q_p ($\Omega^{-1}\,cm^{-2}$)	n_p	
EV300 DF0.14 SR200	3.01	2.58	19.12	49.3	2.29	0.3198	0.61	0.261
EV1800 DF0.14 SR200	3.66	3.05	2.04	6.2	16.52	0.0059	0.78	0.0031
EV1800 DF0.14 SR800	3.22	3.63	1.79	6.5	11.04	0.0023	0.95	0.0019
EV1800 DF0.7 SR200	3.59	3.66	1.6	5.9	14.31	0.0036	0.81	0.0018

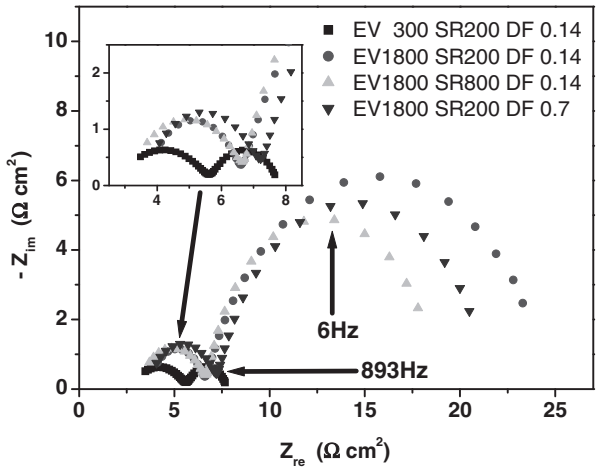

Fig. 4. Nyquist plots of Cu films polished at various electric potentials (EV), down-forces (DF), and speeds of rotation (SR) in H_3PO_4 electrolyte.

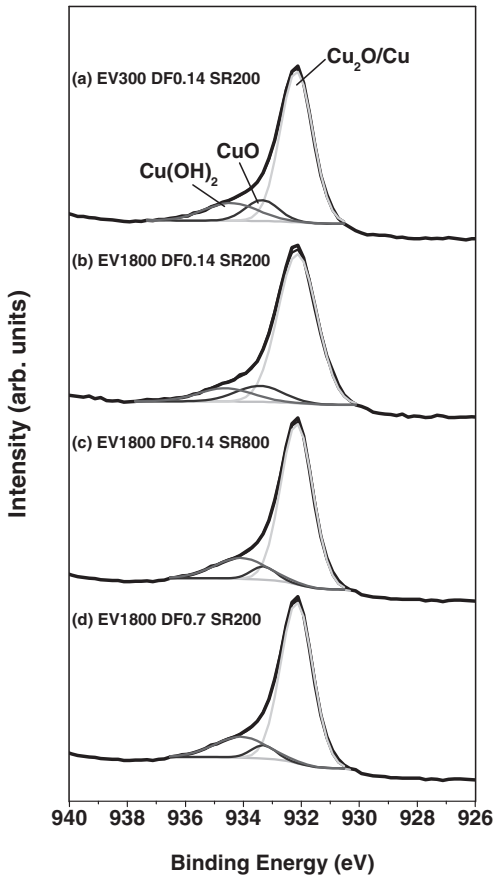

Fig. 5. Cu 2p spectra of Cu films polished at various electric potentials (EV), down-forces (DF), and speeds of rotation (SR) in H_3PO_4 electrolyte.

shows the Nyquist plots of Cu films polished at a high electric voltage of 1800 mV for various down force values and rotating speeds compared to the plot obtained at 300 mV taken from Fig. 3. The fitted values of the circuit components in Fig. 3(d) with Fig. 4 are summarized in Table III. The charge-transfer time-delay decreased markedly when the electric potential was increased from 300 to 1800 mV, indicating that the Cu dissolution rate increased. Moreover, the values of R_{ct} and R_p increased and that of C_p decreased with increasing electric potential, indicating that the thickness of the barrier film increases with increasing electric potential. At the high voltage of 1800 mV, with increases of down force and rotation speed, the charge-transfer time-delay decreased and the Cu dissolution rate increased. R_p decreased with increasing mechanical force, especially for rotation speed, implying that the thickness of the passive film decreased with mechanical force.

The ratio of the variation in R_p from the maximum (denoted as high-level) and minimum (low-level) in the range of each variable from Tables II and III was calculated using

$$M_p = \frac{R_p(\text{high-level})}{R_p(\text{low-level})}, \tag{8}$$

where M_p^{ev} is the ratio of R_p at the highest potential to R_p at the lowest potential at a fixed down force and rotation speed, and M_p^{df} and M_p^{sr} are the ratios of down force and rotation speed, respectively. M_p^{ev} values of 7.21, 8.67, and 14.34 were obtained for DF0.14SR200, DF0.7SR200, and DF0.14SR800, respectively. M_p^{df} values of 0.72 and 0.87 were obtained for EV300SR200 and EV1800SR200, respectively. M_p^{sr} values of 0.34 and 0.67 were obtained for EV300DF0.14 and EV1800DF0.14, respectively. The value of M_p^{ev} is much higher than those of M_p^{df} and M_p^{sr}. This indicates that the increase of potential mainly affects the production rate of the passive film. The values of M_p^{ev} for DF0.7SR200 and DF0.14SR800 are higher than that for DF0.14SR200. The growth rate of the diffusion layer increased with increasing down force or rotation speed probably due to an increase in I_d. The value of M_p^{df} for EV1800SR200 is higher than that for EV300SR200, indicating that the growth rate of the diffusion layer increased with increasing potential. The same result was found for M_p^{sr}.

To investigate surface chemical species, XPS survey spectra of the Cu thin films after ECMP were obtained at various electric voltages, down force values, and rotation speeds, as shown in Fig. 5, for Cu $2p_{3/2}$ spectra. Each of the Cu $2p_{3/2}$ spectra can be decomposed into three peaks at

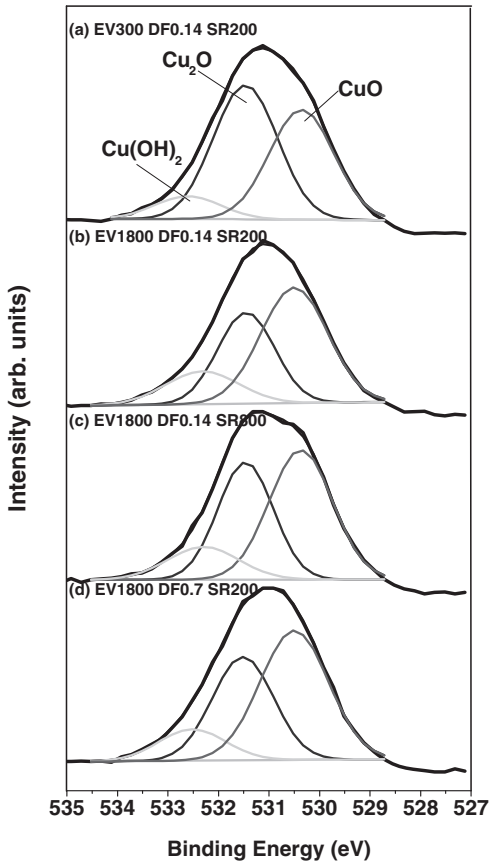

Fig. 6. O 1s spectra of Cu films polished at various electric potentials (EV), down-forces (DF), and speeds of rotation (SR) in H_3PO_4 electrolyte.

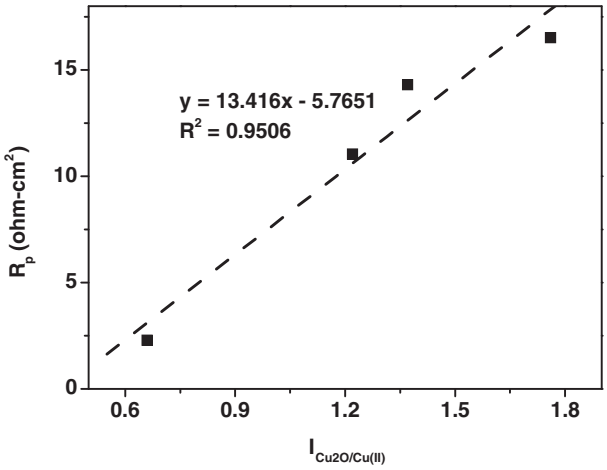

Fig. 7. Relationship between R_p and the intensity ratio of Cu_2O/Cu(II), $I_{Cu_2O/Cu(II)}$, for various ECMP conditions.

932.0 ± 0.2, 933.2 ± 0.3, and 934.1 ± 0.5 eV, which are assigned to Cu/Cu_2O, CuO, and $Cu(OH)_2$, respectively. Figure 6 shows XPS spectra of the O 1s line for the Cu films after ECMP for various conditions. The broad peak of the O 1s spectrum can be decomposed into three peaks at 530.2 ± 0.1, 532.2 ± 0.3, and 531.3 ± 0.1 eV, which are attributed to CuO, $Cu(OH)_2$, and Cu_2O, respectively. The major peak of the O 1s spectrum corresponds to Cu_2O, which is in good agreement with the high-intensity of the Cu_2O peak obtained from the Cu $2p_{3/2}$ spectrum in Fig. 5. Figure 7 shows the relationship between R_p and the intensity ratio of Cu_2O/Cu(II), $I_{Cu_2O/Cu(II)}$, for various ECMP conditions, where Cu(II) includes $Cu(OH)_2$ and CuO. $I_{Cu_2O/Cu(II)}$ increases with increasing R_p, indicating that the R_p increase is due to the growth of the Cu_2O oxide film. XPS spectra of P were also acquired; no phosphorus was found on the Cu film surface after ECMP and electropolishing using a H_3PO_4 electrolyte.[36)]

There appears to be a combination of two processes in Cu ECMP: (i) electrically enhanced metal dissolution and oxide diffusion layer growth and (ii) mechanical wear refreshing the Cu surface of the passive layer. For a constant down force and rotation speed, the Cu removal rate and the thickness of the Cu diffusion film increased with increasing electric potential, as shown in Figs. 2(b) and 3(a). The Cu diffusion layer formed partly due to Cu ions reacting with oxygen or hydroxyl. For a constant electric potential, the Cu removal rate increased slightly and R_p decreased with increasing mechanical force at low electric voltage (300 mV), as shown in Figs. 2(b), 3(b), and 3(c). R_p decreased more significantly with increasing mechanical force at high electric voltage (1800 mV). The Cu oxide film is suppressed by mechanical force, but the effect of the mechanical force on the Cu dissolution rate is lower than that of the electric potential. Therefore, electric potential dominates the Cu dissolution rate at high potential whereas the mechanical force is dominant at low potential. This removal mechanism is greatly different from that observed for CMP or electropolishing.

4. Conclusions

The effects of electric potential and mechanical force during ECMP on the dissolution of a Cu film in H_3PO_4 electrolyte were investigated. The increase of the Cu removal rate at low potential is due to the effect of mechanical force enhanced by electric potential. The increase of the Cu removal rate at high potential is due to the effect of electric potential enhanced by mechanical force. The potentiodynamic measurements show that high electric potential greatly increases I_d, the dissolution rate, and R_p. The effect of mechanical force is not as large as that of electric potential. The value of M_p^{ev} is much higher than those of M_p^{df} and M_p^{sr}. EIS and XPS results reveal that R_p is directly proportional to $I_{Cu_2O/Cu(II)}$, implying that Cu_2O is the major oxide film during ECMP.

Acknowledgments

This work was supported by the National Science Council of Taiwan (Grant Nos. NSC 98-2622-E-006-049-CC2 and NSC 98-2221-E-006-082-MY3). Technical support from the Nation Cheng Kung University is also acknowledged.

1) R. Liu, C. S. Pai, and E. Martinez: Solid-State Electron. **43** (1999) 1003.
2) T. F. Edgar, S. W. Butler, W. J. Campbell, C. Pfeiffer, C. Bode, S. B. Hwang, K. S. Balakrishnan, and J. Hahn: Automatic **36** (2000) 1567.
3) D. Leggett, D. Frye, R. Munzlinger, A. Millaway, J. Serda, P. Burke, M. Evans, B. Kraus, and G. Leggett: PTI Seminars, Inc., I, 1.0 (1998).
4) P. C. Andricacos, C. Uzoh, J. O. Dukovic, J. Horkans, and H. Deligianni: IBM J. Res. Dev. **42** (1998) 567.
5) K. W. Chen, Y. L. Wang, L. Chang, S. C. Chang, F. Y. Li, and S. H. Lin:

Electrochem. Solid-State Lett. **7** (2004) G238.
6) D. Ernur, V. Terzieva, W. Wu, S. H. Brongersma, and K. Maex: J. Electrochem. Soc. **151** (2004) B636.
7) D. Ernur, S. Kondo, and K. Maex: Jpn. J. Appl. Phys. **41** (2002) 7338.
8) N. Chandrasekaran, S. Ramarajan, W. Lee, G. M. Sabde, and S. Meikle: J. Electrochem. Soc. **151** (2004) G882.
9) P. R. Besser and Q. T. Jiang: MRS Proc. **795** (2003) U1.1.
10) F. Q. Liu, T. Du, A. Duboust, S. Tsai, and W. Y. Hsu: J. Electrochem. Soc. **153** (2006) C377.
11) Y. J. Oh, G. S. Park, and C. H. Chung: J. Electrochem. Soc. **153** (2006) G617.
12) J. Huo, R. Solanki, and J. McAndrew: Electrochem. Solid-State Lett. **8** (2005) C33.
13) Y. Hong, D. Roy, and S. V. Babu: Electrochem. Solid-State Lett. **8** (2005) G297.
14) A. Tripathi, C. Burkhard, I. I. Suni, Y. Li, F. Doniat, A. Barajas, and J. McAndrew: J. Electrochem. Soc. **155** (2008) H918.
15) A. S. Brown: IEEE Spectrum **42** (2005) 40.
16) T. M. Kung, C. P. Liu, S. C. Chang, and Y. L. Wang: Nanosci. Nanotechnol. Lett. **1** (2009) 17.
17) S. C. Chang and Y. L. Wang: J. Vac. Sci. Technol. B **22** (2004) 2754.
18) D. Padhi, J. Yahalom, S. Gandikota, and G. Dixit: J. Electrochem. Soc. **150** (2003) G10.
19) D. Tromans and G. Li: Electrochem. Solid-State Lett. **5** (2002) B5.
20) Y. Hong, D. Roy, and S. V. Babu: Electrochem. Solid-State Lett. **8** (2005) G297.
21) A. Tripathi, C. Burkhard, I. I. Suni, Y. Li, F. Doniat, A. Barajas, and J. McAndrew: J. Electrochem. Soc. **155** (2008) H918.
22) P. C. Goonetilleke, S. V. Babu, and D. Roy: Electrochem. Solid-State Lett. **8** (2005) G190.
23) L. Economikos, X. Wang, A. Sakamoto, P. Ong, M. Naujok, R. Knarr, L. Chen, Y. Moon, S. Neo, J. Salfelder, A. Duboust, A. Manens, W. Lu, S. Shrauti, F. Liu, S. Tsai, and W. Swart: Proc. IEEE Int. Interconnect Technology Conf., 2004, p. 233.
24) D. Shirley: Phys. Rev. B **5** (1972) 4709.
25) S. C. Chang, J. M. Shieh, C. C. Hung, B. T. Dai, and M. S. Feng: Jpn. J. Appl. Phys. **41** (2002) 7332.
26) F. H. Giles and J. H. Bartlett: J. Electrochem. Soc. **108** (1961) 266.
27) K. Kojima and C. W. Tobias: J. Electrochem. Soc. **120** (1973) 1202.
28) E. S. M. Sherif, R. M. Erasmus, and J. D. Comins: J. Colloid Interface Sci. **311** (2007) 144.
29) S. Chaudhari, S. R. Sainkar, and P. P. Patil: J. Phys. D **40** (2007) 520.
30) L. Larabi, O. Benali, S. M. Mekelleche, and Y. Harek: Appl. Surf. Sci. **253** (2006) 1371.
31) K. Kojima and C. W. Tobias: J. Electrochem. Soc. **120** (1973) 1026.
32) E. Barsoukov and J. R. Macdonald: *Impedance Spectroscopy: Theory, Experiment, and Applications* (Wiley, Hoboken, NJ, 2005).
33) M. E. Orazem, P. Shukla, and M. A. Membrino: Electrochim. Acta **47** (2002) 2027.
34) H. Ma, S. Chen, B. Yin, S. Zhao, and X. Liu: Corros. Sci. **45** (2003) 867.
35) F. B. Growcock and R. J. Jasinski: J. Electrochem. Soc. **136** (1989) 2310.
36) J. L. Fang and N. J. Wu: J. Electrochem. Soc. **136** (1989) 3800.